Reactive Power Limitation due to Wind-Farm Collector Networks

Jonathon A. Martin   Ian A. Hiskens

Department of Electrical Engineering and Computer Science

University of Michigan

Ann Arbor, USA

Abstract—Type-3 and Type-4 wind turbines are capable of contributing to the reactive power required by wind-farms for supporting grid voltages. However, characterizing the maximum reactive power capability of a wind-farm by summing the individual generator ratings does not account for the effects of voltage variations over the radial collector network and can significantly overestimate the total reactive power production capacity. This paper considers the reactive power produced by a wind-farm in response to a common reactive power set-point Q_{set} that is broadcast to all wind turbines. Analysis shows that a sustained increase in Q_{set} will result in the wind-farm delivering maximal reactive power. Several examples demonstrate that generator voltage limits can significantly curtail the reactive power output requested by the control strategy. This improved characterization of wind-farm reactive power production capabilities, which takes into account collector network voltages, will enable better design and operation of wind-farm reactive power resources, reducing the need for additional shunt capacitors and static synchronous compensators.

Index Terms—Wind energy integration, reactive power, radial networks.

I. INTRODUCTION

Through the use of power electronic converters, type-3 and type-4 wind turbines are capable of controlling their active and reactive power production independently [1], [2]. This has opened up the potential for wind-farm operators to offer reactive power support to the grid utilizing the turbines instead of relying completely on shunt capacitors and Statcoms. In order for this approach to be feasible however, wind-farm operators require an accurate characterization of their wind-farm's reactive power capacity and a control algorithm for exploiting that capacity. One method of estimating this value is to sum together the production capabilities of the individual wind turbines as is done in [3], [4]. However, several studies have found that this method can overestimate the actual reactive power production capacity and that more accurate methods are required [4]–[6]. Existing industry standards specifying the role of wind-farms in reactive power support of the grid, and the testing of those control capabilities are varying and under development [7].

The purpose of this study is to propose a simple method for accurately determining the reactive power production capacity of a radial wind-farm using a common reference signal sent to each of the turbines. This approach naturally identifies the maximum reactive power capacity of a wind-farm. In addition to more accurately characterizing reactive power capabilities, this study also provides insights into the interactions between voltage and reactive power in wind-farm networks.

This study is motivated by results from [5]. There, a common reactive power reference signal Q_{set} was broadcast to all the generators in a radial wind-farm. The local controls at each turbine sought to match the requested reactive power production Q_{set} as long as active, reactive, and voltage limits were not violated. The total reactive power output of the wind-farm can be controlled by varying the common signal Q_{set}, with maximum reactive power attained by increasing Q_{set} until all turbines are at either their voltage limit or their reactive power capability limit. Further increases in Q_{set} beyond that point have no effect on the reactive power output of the wind-farm.

This paper examines this final point of the control process, where all turbines have encountered their capability limits, to determine if it represents the true overall wind-farm limit. By using optimization theory and exploiting the underlying power system structure, it will be shown that this final point does, in fact, give the wind-farm's true reactive power capability limit.

The outline of the paper is as follows. Section II describes the modelling methods and assumptions used in the analysis. Section III formally presents and defines the problem. Section IV justifies the relationships between voltage and reactive power flows. Section V shows why an increase in reactive power production at any of the generators results in an increase in the net reactive power production of the wind-farm. Section VI shows that the final point is the optimal solution within the practical operating region. Section VII concludes the paper.

II. PROBLEM MODELLING AND FORMULATION

This section discusses the general modelling methods and assumptions used throughout this study at both the wind-farm collector network level and the turbine generator level.

A. Collector network model

In this study, only radial network configurations are considered since most wind-farm layouts follow this structure
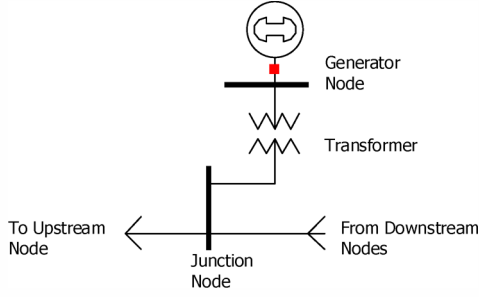
Fig. 1. Basic building block of a radial wind-farm.

Fig. 2. DFIG P-Q capability curve used in this study, based on [10]. Values are normalized according to machine ratings.

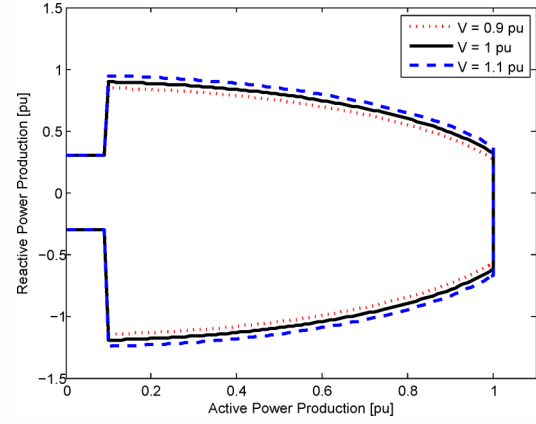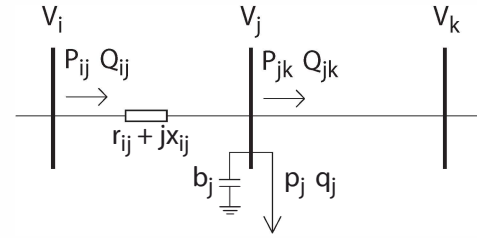Fig. 3. Branch flow formulation. Line impedances (r_{ij}, x_{ij}) and shunt susceptance (b_j) follow the π-model convention.

[4]. It is assumed that the voltage on the high side of the wind-farm's main transformer is fixed. The low side of the main transformer is connected to a medium-voltage collector network arranged in a radial tree structure. The root of the tree is the wind-farm substation. Following a typical distribution network approach, the line end closest to the substation is referred to as the upstream end. Fig. 1 shows a diagram of the basic building block used to lay out radial wind-farm networks. The junction node represents a junction box where a generator connects into the collector network.

Following typical medium-voltage underground cable impedance parameters, the X/R ratio of the lines is rather low and is near unity for the sample networks discussed in this study [4]. Line segments are all about the same length. All transformers have X/R ratios of about ten. The turbine transformers have X values about 100 times greater than the line segment reactances and each of the main substation transformers has an X value about ten times that of the line segments. Line impedances are modeled following the usual π-model, and the transformers are modeled as fixed $R + jX$ impedances.

B. Turbine generator model

This study assumes that the turbines are Type-3 doubly fed induction generators (DFIG). By using a partially rated ac-ac converter, these generators are able to control the rotor current and therefore determine their active and reactive power outputs independently [2].

With this turbine configuration, the reactive power production capability is affected by both the generator voltage and the active power production level [1]. The main limiting factors regulating the active/reactive (P-Q) capability curve are the stator and rotor current limits. A detailed discussion of these limitations can be found in [9], [10]. Generally, the P-Q capability curve has a "D" shape but occasionally manufacturers will supply a rectangular capability curve [8]. In both cases, the turbines are typically capable of operating at a 0.95 power factor leading or lagging at full active power output. The generator voltage also slightly affects the P-Q capability and further discussion can be found in [6], [8], [10].

For the purpose of this study, the turbines are rated at 1.65 MW and are capable of operating between voltage limits of 0.9 pu and 1.1 pu. The P-Q capability curve for the turbines

is shown in Fig. 2. It is assumed that the turbines only experience small slip values in order to discount the limiting effects of the rotor voltage. Additionally, since the stator voltage effects are small, they are ignored in the simulations and the curve with $V = 1$ pu is used to determine the reactive power capability.

C. Power flow formulation

The power flow problem is defined using the DistFlow formulation [11],

$$P_{ij} = P_{jk} + p_j + r_{ij}\frac{P_{ij}^2 + Q_{ij}^2}{V_i^2} \tag{1}$$

$$Q_{ij} = Q_{jk} + q_j + x_{ij}\frac{P_{ij}^2 + Q_{ij}^2}{V_i^2} - b_jV_j^2 \tag{2}$$

$$V_j^2 = V_i^2 - 2(r_{ij}P_{ij} + x_{ij}Q_{ij}) + (r_{ij}^2 + x_{ij}^2)\frac{P_{ij}^2 + Q_{ij}^2}{V_i^2}. \tag{3}$$

In these equations, P_{ij} and Q_{ij} are the active and reactive power flows on line ij in the direction shown in Fig. 3, V_i is the voltage magnitude at node i, and p_j and q_j are the active and reactive power loads at bus j. The values r_{ij} and x_{ij} represent the resistance and reactance of line ij, and b_j represents the shunt susceptance at bus j. Therefore, when the generators are producing power, p and q are negative. Since the nodes in the network are numbered so that bus i is upstream of bus j, the P and Q line flows also tend to be negative
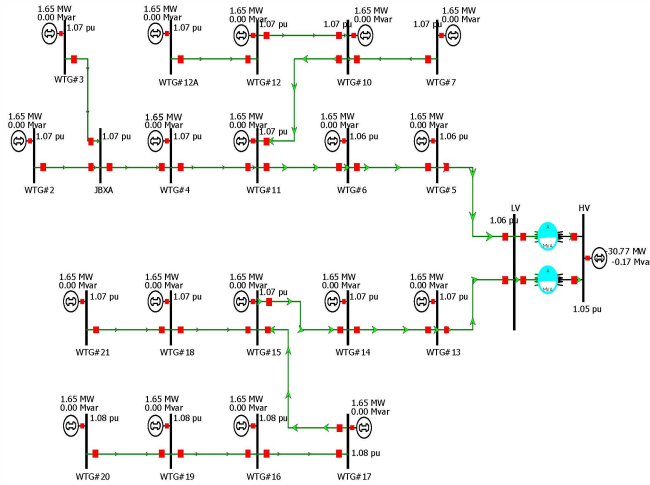
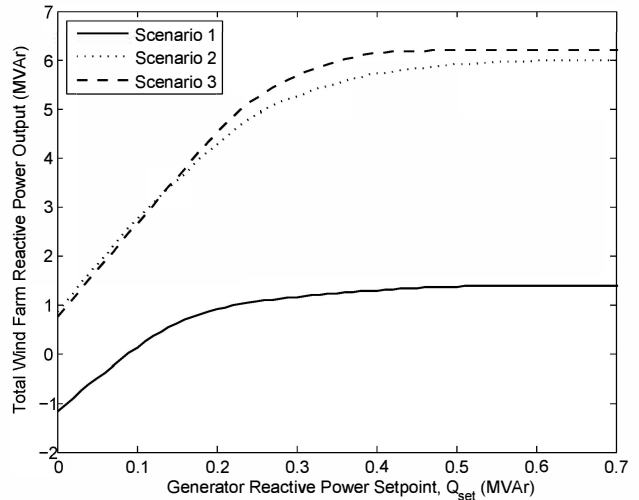Fig. 4. Layout of the example 19 generator wind-farm.

Fig. 5. Response of a wind-farm with 19×1.65 MW generators to a common reference signal for a variety of active power production scenarios.

during production due to power flowing upstream toward the substation at the point of common connection (PCC).

It is assumed that the generator nodes (see Fig. 1) behave as PQ buses during normal operation by regulating their reactive power production to match the reference signal Q_{set}. However, once a voltage limit is encountered, the generator protection overrides the reference signal. The generator node switches to behaving as a PV bus by adjusting its reactive power production to maintain the voltage at its limit, thus avoiding tripping the generator out of service [12].

III. PROBLEM DEFINITION

A. Motivating example

To motivate the discussion of this study, consider an example 19 generator radial wind-farm shown in Fig. 4. Although the generator transformers are not explicitly shown in the layout, they were included in the network model. The relationship between the reactive power output of the wind-farm and the reactive power reference set-point Q_{set} is provided in Fig. 5 for three unique active power production scenarios.

In scenario 1, each of the turbines is at its maximum active power output of 1.65 MW. In scenario 2, the active power production is around half the nameplate capacity of the wind-farm and is concentrated near the ends of each of the branches. In scenario 3, the active power production is slightly greater than in scenario 2 but is concentrated more towards the substation (PCC) at the base of the branches.

In each of the scenarios, three distinct regions can be identified on the curves in Fig. 5 as the common reference signal Q_{set} increases from 0 MVAr. When Q_{set} is around $0 - 0.1$ MVAr the generators are producing almost no reactive power and no capability limits are restricting their response to the reference signal. Therefore, the wind-farm response is approximately linear as expected.[1] The second region is evident

as Q_{set} continues to increase into the range $0.1 - 0.5$ MVAr. The generators at the remote ends of the branches begin to encounter their voltage limits and must reduce their reactive power production in order to avoid over-voltage. This causes the slope of the curve to decrease as fewer generators are able to respond to the increasing Q_{set} control signal. The third region, when Q_{set} reaches about $0.6 - 0.7$ MVAr, is flat. In this region, all of the generators are either at their maximum reactive power output or their voltage limit and are no longer able to increase their reactive power production.

The effect of active power flows throughout the collector network can also be observed in Fig. 5. At $Q_{set} = 0$, none of the generators is producing reactive power and the value of the total reactive power output is only affected by the active power flows through the collector network reactance and shunt susceptance. In the heavily loaded scenario 1, the reactance dominates the system behavior and the wind-farm must absorb reactive power from the transmission grid. In scenarios 2 and 3, the loading is much lighter and the shunt susceptance dominates, allowing the wind-farm to supply reactive power to the grid.

Active power flows also play another role in influencing the reactive power capability of the network. Fig. 5 shows that scenario 3 initially is producing less reactive power than scenario 2 due to greater reactive power losses in the collector network resulting from the larger active power production. However, as reactive power output increased, scenario 3 ended up being able to produce more reactive power than scenario 2 because the active power production was located closer to the PCC and had less influence on the network voltages. This fact could be useful in situations when a wind-farm is required to curtail active power production. Choosing to focus active power curtailment at the remote ends of the branches could not only help to reduce losses, it could also help to maintain greater reactive power control capabilities.

---

[1] In scenarios 2 and 3 where the network is less loaded, the slope is given (approximately) by the number of wind turbines that are in service.

By considering the response of the wind-farm in each of the scenarios, it can be seen that the turbines are only able to increase the net reactive power output of the wind-farm by 2.5 MVAr in scenario 1 and 5.5 MVAr in scenarios 2 and 3 as Q_{set} increased from 0 to 0.5 MVAr. In contrast, a summing approach would estimate that in each scenario the turbines should be capable of producing around $19 \times 0.5 = 9.5$ MVAr neglecting losses. However, losses alone cannot explain this difference. Turbine voltage limits have a much greater impact on the overall performance by causing the elbow of the curves in the range 0.1 to 0.4 MVAr of Fig. 5.

B. Mathematical formulation

As mentioned previously, one of the main aims of this study is to determine whether the maximum reactive power production capability of a wind-farm can be achieved by ramping a common reactive power reference signal Q_{set} that is broadcast to all the turbines. In the previous example, the maximum reactive power was attained at the point where $Q_{set} = 0.6$ MVAr.

In order to analytically examine the performance of this method, the objective can be formulated as the optimization problem,

$$
\begin{aligned}
\max_{q} \quad & Q_{PCC} \\
s.t. \quad & (1),(2) && \forall \text{ lines} \\
& (3) && \forall \text{ nodes} \\
& V^{min} \leq V \leq V^{max} && \forall \text{ generators} \\
& q^{min} \leq q \leq q^{max} && \forall \text{ generators}
\end{aligned}
\qquad (4)
$$

where Q_{PCC} is the reactive power injection of the wind-farm into the grid. It is important to note that Q_{PCC} is defined as flowing in the opposite direction to the reactive power flows in (1)-(3). In this problem, the generator active power production p has been fixed based on wind flow patterns throughout the wind-farm at a given instant in time and the only control variables are the reactive power set-points q of the generators. Since (4) is non-convex, techniques such as trust-region interior-point methods [13] are required to improve the chances of finding the global solution. It will be shown that the proposed control strategy (common reference signal) is capable of identifying the same solution as sophisticated interior-point methods.

In order to gain a better understanding of the feasible region of (4), a simple test case with only two generators is examined. This layout is shown in Fig. 6. Even in this simple network, the problem is non-convex when reactive power limits are ignored. Fig. 7 shows the contour plot of the reactive power at the PCC as a function of the reactive power output from the two generators. While the production values presented in the figure are well outside the limits of an actual wind turbine, this figure demonstrates the complexity of the underlying power flow equations. In the examples used in this paper, the per unit base values are $V_{base} = 34.5$ kV and $S_{base} = 10$ MVA. This means that realistically the generators are only capable
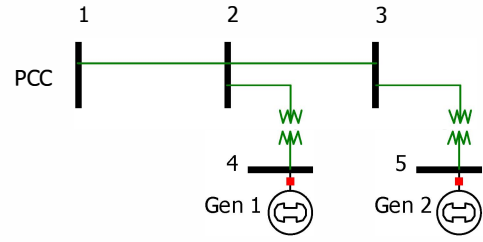

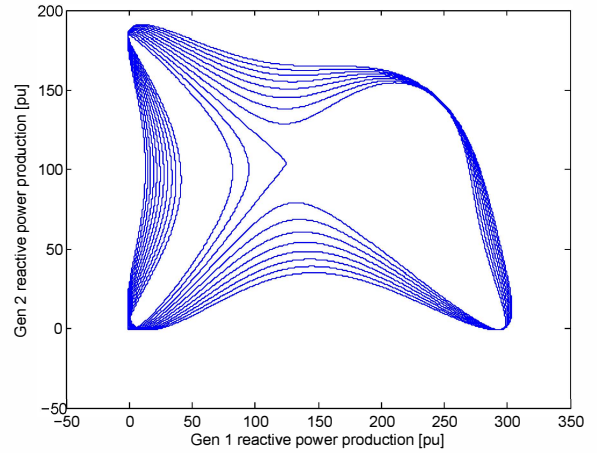Fig. 6. Two generator radial test case.

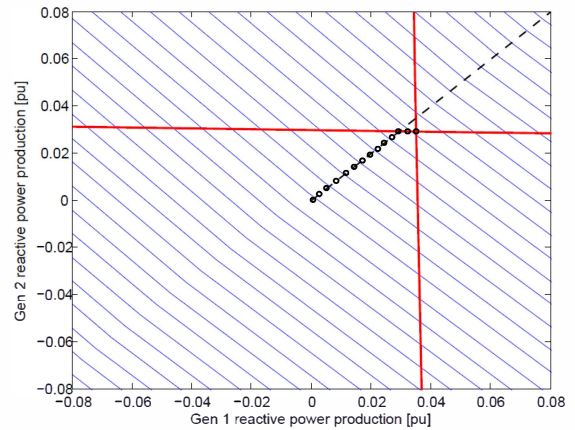Fig. 7. Contour plot of reactive power at the PCC for the two generator case.

Fig. 8. Close up view of contour plot of reactive power at the PCC for the two generator case.

of operating within a reactive power range of about ± 0.15 pu. Fig. 8 shows this more realistic range for the feasible region.

In Fig. 8, it can be seen that the contours of Q_{PCC} are well behaved within normal operating limits. The thicker (red) curves toward the right and top of the figure represent the voltage limits at generators 1 and 2 respectively. Though it is difficult to discern from this perspective, these curves actually bend slightly inward and cause the feasible space to be mildly non-convex. Unfortunately, the implicit nature of the power flow equations (1)-(3) does not allow an explicit expression

of Q_{PCC} or the generator voltages, and solution of these equations requires iterative numerical techniques.

The dashed line starting at $(0, 0)$ and moving toward the upper-right shows the expected response to a sustained increase in the common reference signal Q_{set} if voltage limits are ignored. However, this trajectory intersects the voltage limit on generator 2, which causes the voltage constraint to become binding as Q_{set} increases further. Beyond this point, the actual wind-farm response follows the path indicated by the '∘', with generator 1 following Q_{set} while generator 2 enforces its voltage limit. Once the voltage limit on generator 1 is reached, both generators have binding constraints and no further progress can be made. In this simple case, the deviation from the dashed line is small. However, in larger cases this difference becomes more pronounced.

IV. VOLTAGE PROFILE UNDER A COMMON REFERENCE SIGNAL

The previous section demonstrated how voltage limits function as boundaries on the feasible region. Therefore, in order to show that the final point of the wind-farm response to the common reference signal Q_{set} is a solution to (4), it is important to establish the connection between power flows and voltages. Ideally, a negative monotonic relationship between changes in V_j and q_j should exist so that increasing the reactive power output from a generator will cause the node voltage to rise while decreasing reactive power output will cause the node voltage to drop. This relationship is not true in all general cases, but the following analysis shows that it holds over the feasible region of realistic radial wind-farms.

The structure of (3) indicates that negative power flows P_{ij} and Q_{ij} will cause V_j^2 to be larger than V_i^2. However, in cases where Q_{ij} is positive due to generators absorbing reactive power to remain within voltage limits, the relationship between V_i^2 and V_j^2 is not as clear. In order to show that causing Q_{ij} to become more positive forces V_j^2 lower, consider the linearization of (3) relating changes in $V_j^2 \equiv U_j$ to perturbations in Q_{ij},

$$\delta U_j = -2x_{ij}\delta Q_{ij} + 2\frac{r_{ij}^2 + x_{ij}^2}{V_i^2}Q_{ij}\delta Q_{ij}. \quad (5)$$

This assumes negligible coupling effects between P_{ij} and Q_{ij} from line losses, so that P_{ij} remains unchanged for small fluctuations in Q_{ij}. It also assumes V_i^2 is unaffected by small variations in Q_{ij}. Therefore, these effects have been ignored in the linear approximation. Using this approach, it becomes apparent that δU_j will decrease with increases in δQ_{ij} when

$$2x_{ij} > 2\frac{r_{ij}^2 + x_{ij}^2}{V_i^2}Q_{ij} \quad (6)$$

which can be rewritten,

$$\frac{x_{ij}V_i^2}{r_{ij}^2 + x_{ij}^2} > Q_{ij}. \quad (7)$$

Since $r \approx x$, this simplifies to

$$\frac{V_i^2}{2x_{ij}} > Q_{ij}. \quad (8)$$

In the per unit base of this study, $x_{ij} \in [0.001, 0.01]$ and $V_i \approx 1$. This means that Q_{ij} would have to be greater than $[50, 500]$ in order to violate this constraint. This order of magnitude simply will not happen in a realistic radial wind-farm. Therefore, increasing reactive power production, making Q_{ij} more negative, will cause the downstream voltage V_j to rise. Similarly, decreasing production, making Q_{ij} more positive, will cause V_j to fall.

V. RESPONSE OF PCC REACTIVE POWER TO GENERATOR OUTPUTS

Now that a relationship between reactive power and voltage magnitudes, which bound the feasible region, has been established, a relationship relating wind-turbine reactive power to the objective of (4) should be established. It would be advantageous to show that any increase in reactive power production by any of the generators results in an improvement to the objective of (4). This section presents an argument verifying that this statement is true. A process similar to Section IV is used to show that changes in Q_{jk} and q_j have a positive monotonic relationship to changes in Q_{ij}.

By examining (2), it can be seen that the equation is quadratic in Q_{ij}. Reordering allows (2) to be expressed as

$$\frac{x_{ij}}{V_i^2}Q_{ij}^2 - Q_{ij} + (Q_{jk} + q_j + \frac{x_{ij}P_{ij}^2}{V_i^2} - b_jV_j^2) = 0. \quad (9)$$

The roots of this quadratic can be written,

$$Q_{ij} = \frac{V_i^2}{2x_{ij}}\left(1 \pm \sqrt{1 - \frac{4x_{ij}}{V_i^2}(Q_{jk} + q_j + \frac{x_{ij}P_{ij}^2}{V_i^2} - b_jV_j^2)}\right). \quad (10)$$

Linearizing (10) in terms of either Q_{jk} or q_j results in the same form of equation,

$$\delta Q_{ij} = \mp\left(1 - \frac{4x_{ij}}{V_i^2}(Q_{jk} + q_j + \frac{x_{ij}P_{ij}^2}{V_i^2} - b_jV_j^2)\right)^{-\frac{1}{2}}\delta_{arg}, \quad (11)$$

where δ_{arg} stands for either δQ_{jk} or δq_j. Once again, it is assumed that the small fluctuations in P_{ij}, V_i^2, and V_j^2 due to variations in Q_{jk} or q_j exert minimal influence on Q_{ij}. Based on the form of (11), it can be seen that the expression relating Q_{jk} and q_j to Q_{ij} will be well defined when the term within the square root in (10) is positive. When this term is zero, a bifurcation occurs as the two solutions of (10) coalesce into a single solution. At this point, $Q_{ij} = V_i^2/2x_{ij}$ which is the same form of result expressed in (8). Since it has already been established that $Q_{ij} < V_i^2/2x_{ij}$, (10) solves to the negative square-root solution causing (11) to take on its positive solution. It is therefore clear from (11) that under the condition (8), any change in Q_{jk} or q_j will result in a change of the same sign in Q_{ij}.

This result is important. Consider a solution of the full nonlinear power flow problem presented in (1)-(3). Using (11), an incremental increase in reactive power output at any generator results in an incremental increase in reactive power flowing upstream across the generator transformer to

the junction node. This in turn causes an incremental increase in the reactive power flowing to the upstream junction node. This process continues, eventually reaching the PCC.

This analysis justifies the important observation that no matter the starting point in the feasible region, it can be shown that increasing the reactive power output at any of the generators results in an improvement in the objective function. This relationship can be observed in Fig. 8 by the shape of the contour lines. It underpins analysis of the optimality of the terminal point under the common reference signal Q_{set}.

VI. OPTIMALITY OF THE REFERENCE SIGNAL FINAL POINT

This section establishes that the final state of a wind-farm responding to a sustained increase in the common reference signal Q_{set} is a solution of the optimization problem (4). The final point is a corner point of the feasible region since each of the generators is either at a voltage or reactive power limit. At this point, none of the generators can respond to further increases in the reference signal and the system is at full capacity.

Each increase of the reference signal causes the objective of (4) to improve. This is true based on the reactive power flow relationship presented in Section V and the fact that each of the PQ generator buses is increasing its output at every step. The PV generator buses only decrease their output to circumvent voltage rise which, as was shown in Section IV, is in response to increased power flows. As a result, the objective improves with each increase, up to the corner point of the feasible region. To show optimality, it must be verified that there are no feasible directions out of the corner which could further improve the objective function.

The only way to progress away from the corner point is to reduce the reactive power production of at least one generator. However, as was shown in Section V, this will result in a reduction of the objective. To improve the objective, the reduction at one generator must allow other generators to increase their output enough so that the net result increases the reactive power flowing upstream. All PQ generators are already at their maximum reactive power limit, therefore the increase in production must come from PV generators. Unfortunately, this response is not possible.

In order for the objective to improve, the reactive power flowing upstream from at least one junction node must increase. Consider an arbitrary junction node, as shown in Fig. 1, and assume that the reactive power flowing upstream from this node has increased. Since there are at least two generators in the network, this node is the root for at least two non-intersecting paths to at least two different generators. These paths could be through some combination of generator transformers and lines.

One of these paths is to the generator reducing its reactive power output and so its reactive power flow must decrease. A second path is to a generator which has increased its reactive power output, leading to an increase in its reactive power flow. Based on the result from Section IV, we know that the increased reactive power flowing upstream from this junction

node will cause its voltage to rise. We also know that the increased flow over the second path will cause the voltages downstream along that path to rise. Since the increased reactive power flow must be coming from a voltage limited generator, we encounter a contradiction. Therefore, it is impossible to improve the objective of (4) while moving away from the corner point. Consequently, the final wind-farm state due to increasing the common reference Q_{set} is the desired optimal solution.

VII. CONCLUSION

The paper has considered a simple strategy for controlling the reactive power output of a wind-farm, whereby a common reference signal Q_{set} is broadcast to all operational wind turbines. It has been shown that a wind-farm can be driven to its maximum reactive power capability through a sustained increase in Q_{set}. The influence of generator limits at this maximum point has been explored and optimality of the solution verified. Future work will consider the extension of this approach for providing real-time reactive power operating margins.

REFERENCES

[1] J. G. Slootweg, S. W. H. de Haan, H. Polinder, and W. L. Kling, "Wind power and voltage control" in *Wind Power in Power Systems*, T. Ackermann, Ed., Chichester, England: Wiley, 2005.

[2] S. Müller, M. Deicke, and R. W. De Donker, "Doubly fed induction generator systems for wind turbines," *IEEE Industry Applications Magazine*, vol. 8, no. 3, pp. 26-33, May 2002.

[3] E. H. Camm et al., "Reactive power compensation for wind power plants," in *Proc. 2009 IEEE PES General Meeting*, Calgary, AB, 2009.

[4] A. Ellis and E. Muljadi, "Wind power plant representation in large-scale power flow simulations in WECC," in *Proc. 2008 IEEE PES General Meeting*, Pittsburgh, PA, 2008.

[5] D. F. Opila, A. M. Zeynu, and I. A. Hiskens, "wind-farm reactive support and voltage control," in *Proc. IREP Symposium - Bulk Power System Dynamics and Control - VIII*, 2010.

[6] A. Ahmidi, X. Guillaud, Y. Besanger, and R. Blanc, "A multilevel approach for optimal participating of wind farms at reactive power balancing in transmission power system," *IEEE Systems Journal*, vol. 6, no. 2, pp. 260-269, June 2012.

[7] A. Ellis et al., "Review of existing reactive power requirements for variable generation," in *Proc. 2012 IEEE PES General Meeting*, San Diego, CA, 2012.

[8] A. Ellis et al., "Reactive power performance requirements for wind and solar plants," in *Proc. 2012 IEEE PES General Meeting*, San Diego, CA, 2012.

[9] S. Engelhardt, I. Erlich, C. Feltes, J. Kretschmann, and F. Shewarega, "Reactive power capability of wind turbines based on doubly fed induction generators," *IEEE Trans. on Energy Conversion*, vol. 26, no. 1, pp. 364-372, Mar. 2011.

[10] T. Lund, P. Sørensen, and J. Eek, "Reactive power capability of a wind turbine with doubly fed induction generator," *Wind Energy J. Wiley*, vol. 10, no. 4, pp. 379-394, 2007.

[11] M. E. Baran and F. F. Wu, "Network reconfiguration in distribution systems for loss reduction and load balancing," *IEEE Trans. on Power Delivery*, vol. 4, no. 2, pp. 1401-1407, Apr. 1989.

[12] J. Padrón and A. Lorenzo, "Calculating steady-state operating conditions for doubly-fed induction generator wind turbines," *IEEE Trans. on Power Systems*, vol. 25, no. 2, pp. 922-928, May 2010.

[13] J. Nocedal and S. J. Wright, *Numerical Optimization*, 2nd ed. New York, NY: Springer, 2006.